



Discover Generics

Cost-Effective CT & MRI Contrast Agents



WATCH VIDEO

AJNR

This information is current as of June 22, 2025.

Prenatal Brain MR Imaging: Reference Linear Biometric Centiles between 20 and 24 Gestational Weeks


G. Conte, S. Milani, G. Palumbo, G. Talenti, S. Boito, M. Rustico, F. Triulzi, A. Righini, G. Izzo, C. Doneda, A. Zolin and C. Parazzini

AJNR Am J Neuroradiol 2018, 39 (5) 963-967

doi: <https://doi.org/10.3174/ajnr.A5574>

<http://www.ajnr.org/content/39/5/963>

Prenatal Brain MR Imaging: Reference Linear Biometric Centiles between 20 and 24 Gestational Weeks

 G. Conte,  S. Milani,  G. Palumbo,  G. Talenti,  S. Boito,  M. Rustico,  F. Triulzi,  A. Righini,  G. Izzo,  C. Doneda,  A. Zolin, and  C. Parazzini



ABSTRACT

BACKGROUND AND PURPOSE: Evaluation of biometry is a fundamental step in prenatal brain MR imaging. While different studies have reported reference centiles for MR imaging biometric data of fetuses in the late second and third trimesters of gestation, no one has reported them in fetuses in the early second trimester. We report centiles of normal MR imaging linear biometric data of a large cohort of fetal brains within 24 weeks of gestation.

MATERIALS AND METHODS: From the data bases of 2 referral centers of fetal medicine, accounting for 3850 examinations, we retrospectively collected 169 prenatal brain MR imaging examinations of singleton pregnancies, between 20 and 24 weeks of gestational age, with normal brain anatomy at MR imaging and normal postnatal neurologic development. To trace the reference centiles, we used the CG-LMS method.

RESULTS: Reference biometric centiles for the developing structures of the cerebrum, cerebellum, brain stem, and theca were obtained. The overall interassessor agreement was adequate for all measurements.

CONCLUSIONS: Reference biometric centiles of the brain structures in fetuses between 20 and 24 weeks of gestational age may be a reliable tool in assessing fetal brain development.

ABBREVIATIONS: BPD = biparietal diameter; LLD = latero-lateral diameter; CSA = clivo-supraoccipital angle; FOD = fronto-occipital diameter; GA = gestational age; LCC = length of the corpus callosum; APD = antero-posterior diameter; CCD = cranio-caudal diameter

Prenatal MR imaging plays an important role in the evaluation of the fetal brain, being usually performed as a second-look investigation when suspected brain abnormalities are detected by prenatal sonography. Prenatal MR imaging has been demonstrated to improve the diagnostic accuracy of brain anomalies, leading to changes in clinical management in many cases.¹ Prenatal MR imaging results may also affect parental counseling. In several countries, imaging is

usually performed in the early second trimester (within 24–25 weeks of gestation) because laws and regulations require crucial decisions to be made within such deadline, and additional MR imaging follow-up is not compatible with time constraints.²

Prenatal brain MR imaging, in addition to morphologic assessment, relies on biometry evaluation. In particular, linear biometry is a fundamental step in clinical routine practice. Biometry is relatively easy to assess as far as reference parameters are established. Thus, normative data of the main fetal brain dimensions are necessary to detect possible disorders in brain development. Different studies have reported normative MR imaging biometric data of fetuses in the late second and third trimesters of gestation.^{3–5} In contrast, few studies have reported them in fetuses in the early second trimester, and these had some methodologic limitations: small number of fetuses^{5–7}; inadequate descriptive analysis based on maximum and minimum values rather than on centiles of each measurement^{5,7}; and volumetric measurements difficult to apply clinically (fetal movements during MR imaging acquisition, time-consuming postprocessing analysis).^{6–12}

The purpose of our study was to report centiles of reference MR imaging linear biometric data of a large cohort of fetal brains within 24 weeks of gestation.

Received October 23, 2017; accepted after revision January 1, 2018.

From the Neuroradiology Unit (G.C., G.P., F.T.) and Division of Prenatal Diagnosis (S.B.), Istituto Di Ricovero e Cura a Carattere Scientifico Fondazione Ca' Granda Ospedale Policlinico, Milan, Italy; Department of Clinical Sciences and Community Health (S.M., A.Z.), Laboratory of Medical Statistics, Biometry and Epidemiology "G.A. Maccacaro," and Department of Pathophysiology and Transplantation (F.T.), Università degli Studi di Milano, Milan, Italy; Neuroradiology Unit (G.T.), Padua University Hospital, Padua, Italy; and Fetal Therapy Unit "Umberto Nicolini" (M.R.), Department of Woman Mother and Neonate, and Department of Paediatric Radiology and Neuroradiology (A.R., G.I., C.D., C.P.), Ospedale dei Bambini "V. Buzzi," Milan, Italy.

Please address correspondence to Giorgio Conte, MD, Fondazione IRCCS Ca' Granda Ospedale Maggiore Policlinico, Neuroradiology Unit, Via Francesco Sforza 35, 20122 Milan, Italy; e-mail: giorgioconte.unimed@gmail.com



Indicates article with supplemental on-line tables.



Indicates article with supplemental on-line photos.

<http://dx.doi.org/10.3174/ajnr.A5574>

Table 1: Indications for prenatal MR imaging

Indication for Prenatal MRI	No. of Fetuses (%)
Unclear CNS findings at ultrasound	80 (47)
Extra-CNS disease or malformation	30 (18)
Previous child with a confirmed CNS malformation	59 (35)

MATERIALS AND METHODS

Population

We reviewed the prenatal brain MR imaging data bases of 2 referral centers of fetal medicine, accounting for the examinations performed between 2005 and 2016: three hundred fifty examinations at Istituto Di Ricovero e Cura a Carattere Scientifico Fondazione Ca' Granda Ospedale Maggiore Policlinico (Milan, Italy) and 3500 examinations at Ospedale dei Bambini "Vittore Buzzi" (Milan, Italy). The prenatal MR imaging data bases were approved by the institutional review boards of the 2 hospitals, and all women signed an informed consent for the research use of data.

We collected prenatal brain MR imaging examinations of singleton pregnancies, between 20 and 24 weeks of gestational age (GA), which were performed for the indications reported in Table 1. Exclusion criteria were the following: 1) clear or suspected brain abnormalities at prenatal MR imaging, 2) poor image quality, 3) chromosomal abnormalities, 4) pregnancies complicated by infections, and 5) extra-CNS malformations frequently associated with CNS malformations (eg, cardiac rhabdomyoma). Gestational age was calculated by obstetricians and gynecologists on the basis of the menstrual period and ultrasound criteria and expressed as completed weeks.

Image Acquisition and Analysis

In both hospitals, prenatal MR imaging examinations were performed at 1.5T with the same scanner model (Achieva; Philips Healthcare, Best, the Netherlands) and phased-array abdominal or cardiac coils. Prenatal MR imaging protocols were standard clinical and state-of-the-art, were identical for both hospitals, and included the following: T2-weighted single-shot fast spin-echo multiplanar sections (3- to 4-mm-thick sections; gap = 0.1 mm; TR/TE = 3000/180 ms; in-plane resolution = 1.1-mm²); balanced fast-field echo multiplanar sections (3-mm-thick contiguous sections; TR/TE = 7/3.5 ms; in-plane resolution = 1.5 mm²); T1-weighted fast spin-echo multiplanar sections (5.5-mm-thick sections; TR/TE = 300/14 ms; turbo factor = 3; in-plane resolution = 1.4 mm²); in some cases, T2-weighted 3D fast-field echo sections (1.1-mm-thick sections; TR/TE = 2.5/4.7 ms; in-plane resolution = 1.1 × 1.1 mm²); single-shot fast spin-echo fluid-attenuated inversion recovery sections (4-mm-thick sections; TR/TE = 600/54 ms; in-plane resolution = 1.25 × 3.1 mm²); and diffusion-weighted imaging sections (5.5-mm-thick sections; TR/TE = 1000/90 ms; b factor = 0–600 s/mm²; FOV = 320 × 320 mm, matrix = 128 × 128).

Image analysis was performed on dedicated PACS workstations equipped with professional monitors. All images were independently reviewed for evaluation of biometry with respect to GA by 1 fetal neuroradiologist and 1 resident with >2 years of experience in prenatal MR imaging. In accordance with the method described in previous studies,^{5,13,14} each reader evaluated the following measurements: thecal fronto-occipital diameter (FOD),

thecal biparietal diameter (BPD), length of the corpus callosum (LCC), cerebral FOD, cerebral BPD, width of the atria of the lateral ventricles, mesencephalic antero-posterior diameter (APD), vermian APD, vermian cranio-caudal diameter (CCD), cerebellar latero-lateral diameter (LLD), latero-lateral diameter of the posterior cranial fossa (PCF), pontine APD and pontine CCD, and clivo-supraoccipital angle (CSA). All MR imaging measures were expressed in millimeters, with the only exception being the CSA (degree). The ratio between the LCC and cerebral FOD was also calculated (LCC/cerebral FOD). For details about measurements, see On-line Figs 1A–6B. Each measure was taken twice or thrice on the same or different acquisitions, preferably on balanced fast-field echo images in consideration of their higher spatial resolution (thinner sections) compared with single-shot fast spin-echo T2-weighted images. The average of the measures of each reader was regarded as his best (ie, most reliable) measure. The average of these best measures was used to trace the reference charts.

Statistical Analysis

The lack of precision (random error) of MR imaging assessments was expressed as standard error of measurements (ie, the SD of the measures of the same subject).¹⁵ The difference between the averages of measures made by the 2 assessors (A and B) participating in this study was regarded as an estimate of the difference in their accuracy (systematic error).

The estimates of the size attained at 22 weeks of GA and of the mean weekly increase from 20 to 24 weeks were derived from the following linear model:

$$E(\text{MR trait}) = \mu + \alpha \times s + \beta \times t + \gamma \times s \times t,$$

where $E(\text{MR trait})$ is the expected value of the MR imaging trait, s is 0 for females and 1 for males, $t = \text{GA} - 22$, μ is size attained by females at 22 weeks, α is the "male-versus-female" difference in size attained at 22 weeks, β is mean weekly increase shown by females from 20 to 24 weeks, and γ is the "male-versus-female" difference in an average weekly increase from 20 to 24 weeks.

To trace the reference centiles, we used the CG-LMS method.¹⁶ This expresses the centiles in terms of GA-specific curves called $L(t)$, $M(t)$, and $S(t)$. The $M(t)$ and $S(t)$ curves correspond to the median and coefficient of variation of the MR imaging trait at each age, whereas the $L(t)$ curve allows for the GA-dependent skewness of the distribution of the trait. The value (y) of the MR imaging trait at a given age can be transformed into a SD score (SDS):

$$\text{SDS} = \frac{[y/M(t)]^{L(t)} - 1}{L(t) \times S(t)}.$$

The value $y(p, t)$ of the p th centile at $\text{GA} = t$ is given by $y(p, t) = M(t) \times [1 + z_p \times L(t) \times S(t)]^{1/L(t)}$, where z_p is the standard normal deviate corresponding to probability p .

Centiles were calculated using the software LMS program, Version 1.29 (Medical Research Council, Leicester, UK).

RESULTS

A total of 169 fetuses (23 fetuses of 20 weeks, 73 of 21 weeks, 43 of 22 weeks, 22 of 23 weeks, 8 of 24 weeks) satisfied all the inclusion criteria. One-hundred fifty-nine of 169 fetuses were followed to term and

Table 2: Accuracy and precision of MR imaging measurements

	No. ^a	Mean ^b	B-A ^c	B-A (%) ^d	t Test ^e	P	SEM ^f	CV _{SEM} ^g	r ^h	P
PCF	165	28.61	0.022	0.08	0.17		1.148	4.01	0.059	
Cerebral FOD	168	56.77	-3.258	-5.74	-18.53	<.01	1.611	2.84	0.158	<.05
Cerebral BPD	169	42.12	-1.263	-3.00	-11.68	<.01	0.995	2.36	-0.141	
Vermian APD	167	7.08	0.014	0.20	0.21		0.611	8.64	0.192	<.05
Cerebellar LLD	166	21.81	-1.020	-4.68	-10.41	<.01	0.893	4.09	0.111	
Vermian CCD	168	10.13	-0.934	-9.22	-13.29	<.01	0.644	6.36	-0.004	
CSA	168	72.25	1.020	1.41	1.77		5.278	7.30	0.192	<.05
LCC	152	17.97	0.176	0.98	1.75		0.878	4.89	0.071	
LCC/cerebral FOD (%)	151	31.69	2.252	7.11	11.87	<.01	1.648	5.20	0.238	<.01
Thecal FOD	167	63.47	0.360	0.57	2.97	<.01	1.106	1.74	0.002	
Thecal BPD	169	49.74	0.682	1.37	4.45	<.01	1.410	2.83	0.106	
Mesencephalic APD	118	4.46	0.197	4.41	3.08	<.01	0.490	10.99	0.143	
Pontine APD	159	6.69	-0.074	-1.10	-1.34		0.491	7.34	0.241	<.01
Pontine CCD	158	7.53	-0.384	-5.10	-6.24	<.01	0.547	7.27	0.184	<.05
Lateral ventricles	161	6.76	0.568	8.40	8.15	<.01	0.625	9.25	-0.214	<.01

Note:—SEM indicates standard error of the measurements; APD, antero-posterior diameter; BPD, biparietal diameter; CCD, crano-caudal diameter; CV, coefficient of variation; CSA, clivus-supraoccipital angle; LCC, length of the corpus callosum; LLD, latero-lateral diameter; FOD, fronto-occipital diameter; PCF, latero-lateral diameter of the posterior cranial fossa.

^a The number of observations.

^b Mean of all measurements.

^c Mean difference between assessor B and assessor A (difference in accuracy of assessors A and B).

^d Percentage interassessor difference [$100 \times (B-A) / \text{mean}$].

^e t test for difference in B-A.

^f Measuring error—that is, the SD of the measures of the same fetus (lack of precision).

^g Measuring error expressed as coefficient of variation (%) of ($100 \times \text{SEM} / \text{mean}$).

^h Correlation coefficient between interassessor B-A difference and the mean of the measurements made on a single fetus.

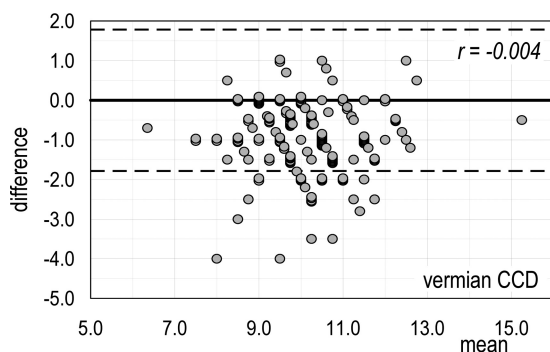


FIG 1. Vermian CCD (the MR imaging trait with the worst percentage disagreement in accuracy between the 2 assessors). Bland-Altman plot of the interassessor B-A difference versus the mean of the measures made on a single fetus. *Dashed lines* are the limits of agreement for the B-A difference: Ninety-five percent of these differences are expected to lie within these limits when the agreement between the 2 assessors is perfect.

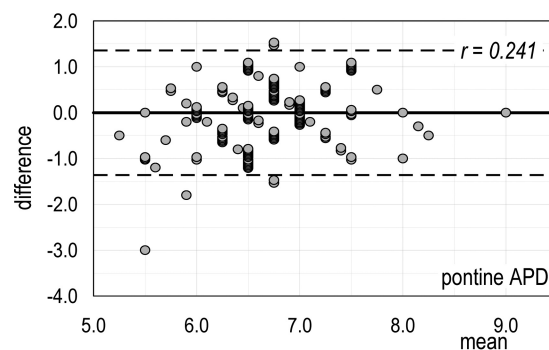


FIG 2. Pontine APD (the MR imaging trait with the highest correlation of disagreement in accuracy between the 2 assessors and size of MR imaging trait). Bland-Altman plot of the interassessor B-A difference versus the mean of the measures made on a single fetus. *Dashed lines* are the limits of agreement for the B-A difference: Ninety-five percent of these differences are expected to lie within these limits when the agreement between the 2 assessors is perfect.

determined to be healthy postnatally. Ten of 169 fetuses were missed at postnatal follow-up, and their sex was unknown because their parents did not want to know the sex at the time of the MR imaging and only head-targeted MR imaging was performed.

Reliability

As reported in Table 2, assessor B provided measures slightly higher than assessor A for most MR imaging traits and slightly lower for the cerebrum (cerebral FOD and BPD), vermis (vermian APD and CCD), and pons (pontine APD and CCD). The interassessor disagreement in accuracy ranged from -9.2% (vermian CCD) to +8.4% (width of the atria of the lateral ventricles). The measuring error ranged from 1.7% (thecal FOD) to 11.0% (mesencephalic APD). A weak positive correlation emerged between the interassessor B-A difference and the mean of the measures made on a single fetus for most traits (maximum

$r = +0.241$, pontine APD). On the contrary, cerebral BPD, vermian CCD, and the width of the atria of the lateral ventricles showed a weak negative correlation (maximum $r = -0.214$).

The Bland-Altman plot for vermian CCD (Fig 1) (ie, the MR imaging trait with the worst percentage disagreement in accuracy between the 2 assessors) shows that 16.1% (27/168) of differences are below the lower agreement limit instead of the expected 2.5%. The Bland-Altman plot for pontine APD (Fig 2) (ie, the MR imaging trait with the highest correlation of disagreement in accuracy between the 2 assessors and size of MR trait) shows that the number of differences within the agreement limits (153/159) is close to the expected one (151/159). Thus, we can conclude that for all the MR imaging traits here considered, both systematic and random errors of measurements can be regarded as negligible. Bland-Altman diagrams for all MR imaging traits are reported in On-line Figs 7).

Table 3: Median and reference limits (5th and 95th centiles) for MR imaging traits between 20 and 24 completed weeks of gestation

	20 Weeks			21 Weeks			22 Weeks			23 Weeks			24 Weeks		
	5th	50th	95th	5th	50th	95th	5th	50th	95th	5th	50th	95th	5th	50th	95th
PCF	23.3	26.3	29.3	24.6	27.8	31.1	25.9	29.3	32.9	27.2	30.8	34.7	28.5	32.4	36.5
Cerebral FOD	46.7	51.2	56.4	50.1	54.8	60.2	53.4	58.4	64.1	56.8	62.0	67.9	60.2	65.5	71.7
Cerebral BPD	36.2	38.7	41.6	37.8	40.9	44.5	39.4	43.0	47.4	40.9	45.2	50.5	42.4	47.3	53.6
Vermian APD	5.5	6.3	7.2	6.0	6.8	7.8	6.4	7.3	8.4	6.8	7.8	9.0	7.2	8.3	9.6
Cerebellar LLD	18.2	19.9	21.8	19.1	21.1	23.4	20.1	22.4	25.0	21.0	23.6	26.6	21.9	24.9	28.3
Vermian CCD	7.7	9.0	10.0	8.3	9.8	10.9	8.9	10.6	11.9	9.5	11.4	12.8	10.1	12.1	13.8
CSA	63.7	71.0	79.9	63.6	71.6	81.5	63.4	72.1	83.2	63.2	72.7	85.0	63.1	73.2	86.8
LCC	13.3	15.3	17.1	14.7	17.1	19.2	16.0	18.9	21.4	17.3	20.7	23.6	18.6	22.5	25.8
LCC/cerebral FOD (%)	27.3	29.9	32.5	27.8	31.1	34.3	28.3	32.3	36.1	28.7	33.5	38.0	29.1	34.7	39.9
Thecal FOD	53.4	57.5	62.1	56.7	61.3	66.6	60.0	65.2	71.2	63.2	69.0	75.7	66.4	72.8	80.4
Thecal BPD	42.1	45.7	49.9	44.4	48.3	52.9	46.7	50.9	56.0	49.0	53.6	59.1	51.3	56.2	62.1
Mesencephalic APD	3.6	4.4	5.2	3.7	4.5	5.2	3.8	4.5	5.3	3.8	4.6	5.3	3.9	4.6	5.3
Pontine APD	5.5	6.2	6.9	5.7	6.5	7.3	6.0	6.8	7.7	6.3	7.1	8.0	6.5	7.4	8.4
Pontine CCD	6.3	7.1	7.9	6.5	7.4	8.3	6.7	7.7	8.7	6.8	8.0	9.0	7.0	8.2	9.4
Lateral ventricles	5.7	7.0	8.4	5.3	6.8	8.4	5.0	6.6	8.4	4.7	6.4	8.5	4.5	6.3	8.5

Note:—APD indicates antero-posterior diameter; BPD, biparietal diameter; CCD, cranio-caudal diameter; CSA, clivus-supraoccipital angle; LCC, length of the corpus callosum; LLD, latero-lateral diameter; FOD, fronto-occipital diameter; PCF, latero-lateral diameter of the posterior cranial fossa.

Encephalic Growth

At 22 weeks of gestation, the MR imaging traits under study attained a size ranging from 4.5 mm (mesencephalic APD) to 65.2 mm (thecal FOD). The CSA was 72.5°, and the LCC/cerebral FOD ratio was 31.7%. The average weekly increase from 20 to 24 weeks was highly significant for all traits except for CSA and mesencephalic APD and ranged from 0.31 mm/week (pontine APD and CCD) to 3.81 mm/week (thecal FOD). The growth rate (ie, weekly increase/size at 22 weeks) ranged from 0.69% (CSA) to 9.22% (LCC). The only MR imaging trait that was found to decrease with increasing GA was the width of the atria of the lateral ventricles (-0.20 mm/week, -3.0%). Details are reported in On-line Table 1.

Difference between Sexes in Encephalic Growth

At 22 weeks of gestation, male fetuses are already larger for all MR imaging traits, with only the exception of the vermian APD and LCC/cerebral FOD ratio. The maximum difference was observed in the PCF, where males are larger than females by 5.2%. As for the weekly increase of MR imaging traits, males appeared to grow faster than females from 20 to 24 weeks of GA for 9 of the 15 MR imaging traits under study, with a maximum of 17.9% for PCF (On-line Table 3). Possibly because of the shortness of the GA interval considered, none of the differences between the sexes in growth velocity were significant. Details are given in On-line Tables 2 and 3.

Reference Centiles

The sex differences reported above, though extremely interesting from an ontogenetic point of view, were not large enough to suggest the need for different reference charts for females and males. Thus, MR imaging traits were fitted with a CG-LMS model independent of sex. In the short GA interval under study, $M(t)$ and $S(t)$ were assumed to change linearly with GA, whereas $L(t)$ was assumed to be constant. The use of more flexible CG-LMS models did not improve the goodness of fitting. All the diameters of the cerebrum, cerebellum, and theca were found to have a positively skewed distribution, as well as the CSA. The remaining MR imaging traits were negatively skewed. The coefficient of variation appeared to increase slightly with increasing GA in all MR imaging traits, with the only exception being the cerebral FOD and mesencephalic APD. De-

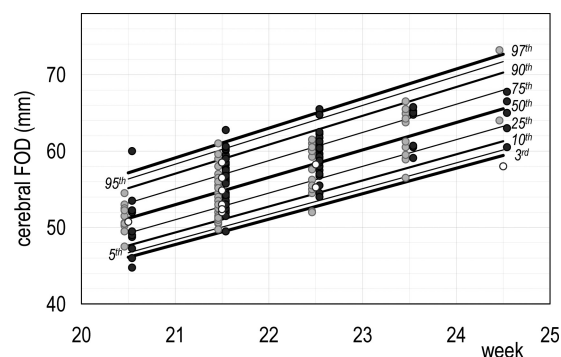


FIG 3. Reference chart for cerebral FOD growth: a whole set of computed centiles (3rd, 5th, 10th, 25th, 50th, 75th, 90th, 95th, 97th) with observed values. Females are denoted by light gray dots, males by dark gray dots, and fetuses of sex unknown by white dots.

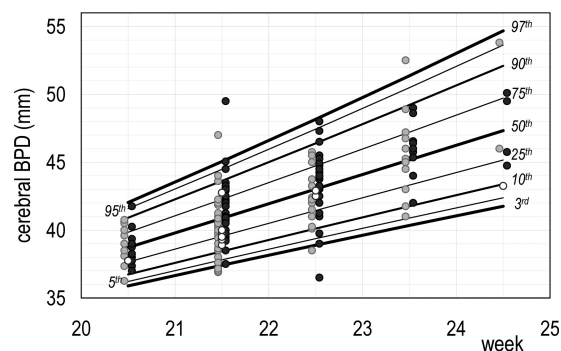


FIG 4. Reference chart for cerebral BPD growth: a whole set of computed centiles (3rd, 5th, 10th, 25th, 50th, 75th, 90th, 95th, 97th) with observed values. Females are denoted by light gray dots, males by dark gray dots, and fetuses of sex unknown by white dots.

tails are reported in On-line Table 4. GA-dependent reference centiles (5th, 50th, and 95th centiles) are given in Table 3. Figs 3 and 4 show growth charts of the cerebral FOD and BPD. The growth charts of all MR imaging traits are given in On-line Fig 8.

DISCUSSION

We provided reference linear fetal brain measurements that can be used for clinical fetal MR imaging on a single-case basis. In particular, our

study focused on GAs between 20 and 24 weeks because in many countries, crucial decisions such as pregnancy termination are possible only in the early second trimester because of laws and regulations.² Until now, most of the MR imaging fetal studies in the literature have referred to normative biometric data published by Parazzini et al in 2008⁵ to examine fetuses younger than 24 weeks of gestation. In this study, the authors did not calculate centiles but provided the minimum and maximum of each measured parameter.⁵ In our study, we conspicuously enlarged that population by doubling the number of fetuses younger than 24 weeks of gestation, and we applied a CG-LMS method to trace the reference centiles. Comparing our data with those by Parazzini et al, we observed differences for some reference limits of supratentorial measurements (eg, cerebral FOD and BPD), while no substantial difference was noted in reference limits of subtentorial structures (eg, vermian diameters and cerebellar LLD). However, our study is not directly comparable with that of Parazzini et al because of the different statistical methods used for the analyses.

We implemented the measurements by Parazzini et al,⁵ and we also added the PCF, CSA, pontine APD, pontine CCD, and mesencephalic APD. Furthermore, we provided the LCC/cerebral FOD ratio. The PCF and CSA may be useful for the assessment of posterior fossa malformations, accounting for dimensional anomalies such as Dandy-Walker malformation and closed neural tube defects.^{13,17} The diameters of the pons (ie, pontine APD and CCD) and the mesencephalic APD may be useful for the assessment of malformations involving the brain stem, such as pontocerebellar hypoplasia, molar tooth malformation, and diencephalic-mesencephalic junction dysplasia. The LCC/cerebral FOD ratio may help in assessing midline malformations, such as isolated mild-to-moderate forms of corpus callosum hypoplasia, an entity that often cannot be reliably assessed by simple visual judgment.

Data about interassessor agreement showed that almost all measurements are, in a sense, objective and independent of the idiosyncrasies of the assessor. The mesencephalic APD showed the highest variability (Table 2). This can be explained by the difficulty in obtaining a suitable orbitomeatal plane (only in 118 of 169 fetuses in our group) and in further delineating the interpeduncular fossa and the mesencephalic tectum. The vermian APD and CCD showed a high variability because of their small size and the difficulty in delineating the fastigium of the fourth ventricle. In agreement with Parazzini et al,⁵ we decided to measure the LCC as the distance between the anterior and posterior inner surfaces because they are better delineated than the outer ones due to the marked contrast with the contiguous CSF. However, as reported in Table 2, in 17 of the 169 fetuses, the LCC could not be measured by the 2 assessors because an exact midsagittal plane was not available.

The main purpose of this work was obviously to provide reliable reference limits that can be used in daily clinical practice; however, we took the opportunity of such measurement collection to acquire information about physiologic cerebral and cranial growth based on linear measurements.

The main limitation of our study is that the fetuses were not homogeneously distributed across the GAs of interest and we included only 8 fetuses at 24 weeks of GA. However, the CG-LMS method calculated the growth curves and the reference limits for

each GA, taking into account all data collected, under the sensible assumption that the growth rate does not change suddenly from one week of gestation to the subsequent week.

CONCLUSIONS

We provided new reference limits of the biometric measurements used for the MR imaging assessment of the fetal brain between 20 and 24 weeks of gestation.

REFERENCES

- Griffiths PD, Bradburn M, Campbell MJ, et al; MERIDIAN collaborative group. **Use of MRI in the diagnosis of fetal brain abnormalities in utero (MERIDIAN): a multicentre, prospective cohort study.** *Lancet* 2017;389:538–46 [CrossRef Medline](#)
- Conte G, Parazzini C, Falanga G, et al. **Diagnostic value of prenatal MR imaging in the detection of brain malformations in fetuses before the 26th week of gestational age.** *AJNR Am J Neuroradiol* 2016;37:946–51 [CrossRef Medline](#)
- Tilea B, Alberti C, Adamsbaum C, et al. **Cerebral biometry in fetal magnetic resonance imaging: new reference data.** *Ultrasound Obstet Gynecol* 2009;33:173–81 [CrossRef Medline](#)
- Ber R, Bar-Yosef O, Hoffmann C, et al. **Normal fetal posterior fossa in MR imaging: new biometric data and possible clinical significance.** *AJNR Am J Neuroradiol* 2015;36:795–802 [CrossRef Medline](#)
- Parazzini C, Righini A, Rustico M, et al. **Prenatal magnetic resonance imaging: brain normal linear biometric values below 24 gestational weeks.** *Neuroradiology* 2008;50:877–83 [CrossRef Medline](#)
- Kyriakopoulou V, Vatansever D, Davidson A, et al. **Normative biometry of the fetal brain using magnetic resonance imaging.** *Brain Struct Funct* 2017;222:2295–2307 [CrossRef Medline](#)
- Moreira NC, Teixeira J, Themudo R, et al. **Measurements of the normal fetal brain at gestation weeks 17 to 23: a MRI study.** *Neuroradiology* 2011;53:43–48 [CrossRef Medline](#)
- Clouchoux C, Guizard N, Evans AC, et al. **Normative fetal brain growth by quantitative in vivo magnetic resonance imaging.** *Am J Obstet Gynecol* 2012;206:173.e1–8 [CrossRef](#)
- Corbett-Detig J, Habas PA, Scott JA, et al. **3D global and regional patterns of human fetal subplate growth determined in utero.** *Brain Struct Funct* 2011;215:255–63 [CrossRef Medline](#)
- Limperopoulos C, Tworetzky W, McElhinney DB, et al. **Brain volume and metabolism in fetuses with congenital heart disease: evaluation with quantitative magnetic resonance imaging and spectroscopy.** *Circulation* 2010;121:26–33 [CrossRef Medline](#)
- Scott JA, Habas PA, Kim K, et al. **Growth trajectories of the human fetal brain tissues estimated from 3D reconstructed in utero MRI.** *Int J Dev Neurosci* 2011;29:529–36 [CrossRef Medline](#)
- Grossman R, Hoffman C, Mardor Y, et al. **Quantitative MRI measurements of human fetal brain development in utero.** *Br J Anaesth* 2006;33:463–70 [Medline](#)
- Woitek R, Dvorak A, Weber M, et al. **MR-based morphometry of the posterior fossa in fetuses with neural tube defects of the spine.** *PLoS One* 2014;9:e112585 [CrossRef Medline](#)
- Garel C. **Fetal cerebral biometry: normal parenchymal findings and ventricular size.** *Eur Radiol* 2005;15:809–13 [CrossRef Medline](#)
- Weir JP. **Quantifying test-retest reliability using the intraclass correlation coefficient and the SEM.** *J Strength Cond Res* 2005;19:231–40 [Medline](#)
- Cole TJ, Green PJ. **Smoothing reference centile curves: the LMS method and penalized likelihood.** *Stat Med* 1992;11:1305–19 [CrossRef Medline](#)
- D'Addario V, Pinto V, Del Bianco A, et al. **The clivus-supraocciput angle: a useful measurement to evaluate the shape and size of the fetal posterior fossa and to diagnose Chiari II malformation.** *Ultrasound Obstet Gynecol* 2001;18:146–49 [CrossRef Medline](#)